R. & M. No. 2530
(8852)
A.R.C. Technical Report

MINISTRY OF SUPPLY

AERONAUTICAL RESEARCH COUNCIL
REPORTS AND MEMORANDA

An Experimental Investigation into the Suitability of a Corrugated Construction Wing for a Laminar-Flow Aerofoil

By

J. C. KING, M.Sc. (Eng.), A.F.R.Ae.S.

LONDON: HIS MAJESTY'S STATIONERY OFFICE
1951
PRICE 9*s* 6*d* NET

An Experimental Investigation into the Suitability of a Corrugated Construction Wing for a Laminar-Flow Aerofoil

By

J. C. KING, M.Sc. (Eng.), A.F.R.Ae.S.

COMMUNICATED BY THE PRINCIPAL DIRECTOR OF SCIENTIFIC RESEARCH (AIR)
MINISTRY OF SUPPLY

Reports and Memoranda No. 2530

January 1945*

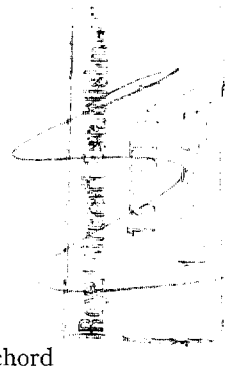

Summary.—This report describes a detailed experimental investigation into the structural features of a 6-ft chord wing specimen having thick skin reinforced by spanwise corrugations. The tests included surface distortion, proof and ultimate tests on the specimen and compression tests on two panels. A short length of parallel specimen was used with a simplified test rig built for the purpose.

These tests showed that for this specimen, provided the wing can be made smooth in the first place, it will not be adversely affected by loads imposed in service. The major portion of the surface distortion in flight will be due to the aerodynamic suction ; the effect of direct and shear stresses being negligible.

In the ultimate tests failure was due to elastic instability of the skin and corrugations at a compressive stress of 11·1 t/sq in. This compares favourably with the compressive stress at failure of the panels, which, when corrected for the shear stress present in the wing, reduces to 11·3 t/sq in.

1. *Introduction.*—Following the successful development of laminar-flow wing sections has come the structural problem of designing and making an aircraft wing suitable for these sections. In the first place this involves the manufacture of a wing which, when completed, is sufficiently smooth to maintain laminar flow back to the position of minimum pressure. A wing of this type must also maintain its smooth surface when subject to the loads arising during ordinary gusts and mild manoeuvres while the aircraft it is supporting flies at maximum level or cruising speeds. Further, after a severe manoeuvre no permanent skin distortions must remain that would distract from the wing's laminar-flow properties at maximum level or cruising speeds.

Some types of construction are likely to prove more suitable for smooth wings than others, and an extensive programme of tests has been planned on specimens of the various types of construction to determine their suitability as smooth wings. The present report deals with a specimen having a thick skin reinforced with spanwise corrugations. There are several advantages in this type of construction from the smooth wing aspect. The corrugations provide an almost continuous stiffening support for the skin, added to which the combination of both is able to take the bending and shear loads with a reasonable degree of efficiency.

The specimen referred to was a 6-ft chord parallel section of a wing and was submitted for loading tests after it had been tested in the wind tunnel at the National Physical Laboratory. The tests were made to determine whether the wing satisfied the conditions required of a laminar-flow wing as outlined above. The wind-tunnel tests made at the N.P.L. are reported in Ref. 1.

For convenience this report is divided into three parts as follows :—

Part I .. Description of Specimen, Experimental Investigation and Summary of Results.
Part II .. Comments on the Aerodynamic Efficiency of the Wing.
Part III .. Comments on the Structural Features of the Wing.

* R.A.E. Report S.M.E. 3291, received 23rd July, 1945.

PART I

Description of Specimen, Experimental Investigation and Summary of Results

2. *Description of Specimen.*—The original wind-tunnel specimen was a 5-ft long length of parallel specimen of 6-ft chord having a NACA 66–2–216 aerofoil section, that is an aerofoil having a 16 per cent. thickness-chord ratio and a 2 per cent. camber with the maximum suction occurring at the 60 per cent. chord position. The specimen used for the loading tests comprised that part of the wind-tunnel specimen forward of the rear web at the 60 per cent. chord position. This was suitably adapted for the loading tests. Details of the construction and method of manufacture of the complete specimen and of the modifications necessary to make it suitable for test are given in the following three sections.

2.1. *Type of Construction.*—A cross-section of the wing showing details of the construction is given in Fig. 1. The wing comprised a corrugated load-carrying box section to which were secured leading and trailing-edge portions. The box section extended from the 5 to the 60 per cent. chord position and was made up of corrugated top and bottom panels joined by thin dural webs reinforced with stiffeners. Ribs were spaced at 15-in pitch and were made up from two preformed channel sections joined on the chord line of the section. The corrugations were originally attached to the skin by No. 4 Parker-Kalon self-tapping screws 3/16-in long at 3-in pitch inserted internally. These were of such a length that the ends did not protrude above the skin surface and the resulting holes were filled with a suitable filler. When it was decided to make loading tests on the wing as well as wind-tunnel tests, one externally driven No. 6 Parker-Kalon self-tapping screw was inserted between each of the internally inserted screws. These screws were of such a length that they passed right through the skin and the corrugations. Further screws had to be inserted during the course of the tests owing to failure of the internally inserted screws. Details of these are given in section 5.4. The leading edge, which had no ribs, was formed from 18 s.w.g. dural.

The material of construction used was dural to Specification D.T.D. 390. The trailing edge was a dummy structure provided for the wind-tunnel tests and not intended to be representative of a trailing edge that might be used on an aircraft.

2.2 *Method of Manufacture.*—The first process in the manufacture of the specimen was to build up the top and bottom skin panels complete with corrugations. The outer skin of each panel was first rolled to profile dimensions on a three-roller bending machine in which the position of the third roller was cam-operated to give the desired shape (Fig. 2a). The skin so formed was then clamped in an accurately made jig complete with the corrugated strips previously rolled from flat strip. The type of jig used is illustrated in Fig. 2b. This removes any discrepancies in the skin profile which could not be removed by rolling. It should be noted that the arrangement of the corrugations in the jig was such that relative slip could occur, thus permitting the skin to take up its correct shape. With this assembly still in the jig the corrugations were then screwed to the skin and the rib diaphragms screwed to the corrugations, using shims if necessary between the diaphragm flanges and the corrugations. After all the diaphragms had been secured to the panels the assembly was removed from the jig, as the rib diaphragms then served to hold the panels to the shapes of the jig surfaces in which they had been built up.

The two skin sub-assemblies were then joined together by the attachment bolts passing through their common flanges, and the front and rear webs assembled. The leading edge was rolled to the correct curvature and shape and then assembled onto the wing. The construction of the trailing-edge portion then followed, but as this part of the wing was a dummy structure the method of manufacture will not be described in detail here.

2.3. *Modifications to Specimen for Test.*—For the purpose of these tests the trailing edge was removed from the specimen, as the smoothness of this part of the wing under load is not critical, since it is aft of the estimated transition point. The specimen was then reinforced at each end and fitted with loading attachments to enable internal pressure, bending and torsion loads to be applied. An outline drawing showing the modified specimen and the end attachments is given in Fig. 3. It will be seen that the general scheme of modification was to reinforce the ends of the specimen by diffuser plates, to fit end bulkheads for the application of torsion and sealing of the specimen and vertical beams for the application of bending load. These were secured to the specimen by cast iron attachment brackets bolted to these fittings and to the specimen. Suitable connections were provided in the rear web for fitting air pressure supply and measuring lines.

3. *Range of Investigation.*—After modification of the wing and before any loading was applied, measurements were made of the initial shape of the specimen. Then followed a number of tests on the end conditions of the specimen to ensure that end planes of the specimen remained plane under load. From these tests it was possible to determine the best position for the loading point in a fore-and-aft direction. A badly located loading point would have lead to severe distortion and twisting of the end bulkheads which, in turn, would have resulted in part of the specimen taking more than its representative share of the bending moment. The three major series of tests detailed below were then made.

Series A .. Distortion tests to determine the amount of distortion of the wing surface which would occur in flight under a normal acceleration of $n = 2g$.

Series B .. Proof tests to determine the load required to produce permanent distortions large enough to affect the aerodynamic efficiency of the wing.

Series C .. Ultimate test to determine the failing load of the specimen.

After the completion of these tests compression tests were made on two panel specimens, one cut from the top surface and the other from the bottom surface of the wing.

3.1. *Loading Conditions.*—The wing section was designed to an ultimate factor of 6 with a wing loading of 40 lb/sq ft, the appropriate data required for design purposes being obtained from estimates prepared for a complete aircraft with a similar wing structure to that of the specimen.

The design loads at factor $n = 1g$ were as follows.

Bending moment = 222,000 lb in.

Torsion = 41,250 lb in (Test torsion = 82,500 lb in).

Owing to the method of test both these loads had to be modified to make the test as representative as possible. The method of applying the bending load (*see* section 4.1) was such as to produce a tension load in the bottom surface less than the compression load in the top surface. Hence as the compression surface was the critical surface as far as buckling and distortion were concerned the loading was adjusted so that the compression in the top surface at factor $n = 1g$ was equal to the load arising from the application of the unit factored bending moment acting alone. The torsion load was increased to the test value given above to produce a higher shear stress in the skin than would arise from the torsion alone. In this way allowance was made for the shear stress in the top skin near the webs arising from the vertical shear loads.

Two test cases were used for the loading, in both of which the bending and torsion loads at factor 1 were the same as those given above and increased uniformly with factor. The difference between the cases was determined by the internal pressure loading as described below.

Gust Case.—This case represented an increase in normal acceleration from 1 to $2g$ occurring at the maximum level speed of 330 m.p.h. (E.A.S.) and arising from a change of incidence due to a gust. It will be seen from Fig. 4 that the change of maximum pressure coefficient from $-0{\cdot}59$ at $C_L = 0{\cdot}141$, which corresponds to $V_{max.}$ level, to $-0{\cdot}64$ at $C_L = 0{\cdot}282$ which corresponds to a factor of $2g$ at the same speed, is small. The resulting pressure change is from

164 lb/sq ft to 178 lb/sq ft, and hence for test purposes the internal pressure was kept constant above unit factor at 170 lb/sq ft. The reason for the difference between the top and bottom surface pressure coefficients at $0 \cdot 6c$ not doubling when the lift coefficient is doubled is that even at zero lift there is a large difference in pressure at these two points. This is further illustrated by the pressure distributions corresponding to $n = 1g$ and $n = 2g$ shown in Fig. 5. in which a comparison between the true and the test chordwise pressure distribution is also shown. It should be remarked that the gust velocity normal to the flight path required to give the change in lift coefficient described above is 13·5 ft/sec. This is approximately half the specified stressing maximum laid down in Ref. 2, Chapter 203.

Proof Case.—This case was specially chosen to be reasonably representative and to give a normal type of load deflection graph, for easy interpretation,instead of the peculiar shape obtained with the gust case load (*see* Fig. 15) due to the discontinuity in the load factor-pressure curve. As the maximum velocity coefficient and hence the maximum pressure coefficient changes with C_L as indicated for this aerofoil in Fig. 4 it was decided that the proof case must be based on a constant lift coefficient

A constant lift coefficient of 0·47 was therefore chosen, as precise data existed for this value of C_L, and a larger value would correspond to a very non-uniform pressure distribution across the working section of the type shown in Fig. 5 for $C_L = 1 \cdot 2$, which could not have been represented on test. Any decrease in this coefficient would have required speeds in excess of the permissible diving speed at the proof load. The chosen C_L of 0·47 corresponds to a speed of 182 m.p.h. (E.A.S.) at factor 1 and a pressure of 60 lb/sq in, which corresponds to a maximum pressure coefficient of $-0 \cdot 70$. The resulting speed at the design proof load of $0 \cdot 75 \times 6g = 4 \cdot 5g$ is $\sqrt{4 \cdot 5} \times 182 = 386$ m.p.h. (E.A.S.) which is less than the estimated diving speed of 430 m.p.h. ($1 \cdot 3\ V_{max.}$). Hence the case represents a reasonable flight loading at all factors.

Chordwise pressure distribution diagrams for this case are given in Fig. 5.

3.2. *Distortion and Deflection Measurements.*—The various measurements taken both initially and during the course of the tests are indicated below; a description of the appropriate apparatus is given in Section 4.2. Details of the particular measurements taken in each test are given in section 3.3.

(a) Profile gauge measurements at chordwise sections 1 to 7 on top and bottom surfaces.

(b) Curvature gauge measurements near chordwise sections 2, 4 and 6 on top and bottom surfaces.

(c) Traverse gauge measurements at corrugation crests 2 and 14 and troughs 3 and 15.

(d) ' Step ' Measurements of the difference in level of the two skins at the leading-edge skin joint on the top surface at eight sections along the span.

(e) Dial board measurement of the distortion of the skin at the crests and troughs of corrugations relative to the front and rear webs at chordwise sections A, B and C.

(f) Deflection measurements of the bending and twist of the specimen over the test length.

(g) Measurements of the horizontal closure between the end bulkheads.

The location of the various sections and the position of the ' crest ' and ' trough ' of corrugations are illustrated in Fig. 6.

3.3. *Test Programme.*—Details of the test programme are given in the following table. In some of the tests certain loads were omitted. These omissions are noted in the remarks column under ' Loading Conditions '.

After completion of the tests listed in the table, material control tests were made by Materials Department, Royal Aircraft Establishment, on specimens cut from the skin and corrugations of the compression surface.

Test			Loading Conditions			Measurements
Series	Title	No.	Case	Factor	Remarks	Standard (*see* section 3.2)
	Initial Shape Measurements.		—	—	No load	(*a*) Profile (*b*) Curvature (*c*) Traverse (*d*) ' Step '
	Measurements of End Conditions.		Special	2	Bending and pressure only.	(*g*) Horizontal closure
A	Distortion up to 2*g*.	I.100 II.300 III.100 IV.100	Gust ..	2	Pressure only. Pressure and bending only. Pressure and torsion only. Pressure, bending and torsion.	(*e*) Dial board measurements.
B	Proof Tests	V.100 V.200 V.300 V.400 V.500	Proof ..	3·5 3·5 3·5 4 5	Pressure, bending and torsion.	(*e*) Dial board measurements. (*f*) Deflection measurements. *
C	Ultimate Test ..	VI.100	Proof ..	5·85 (Failure)	Bending and torsion only.	(*f*) Deflection. measurements
	Panel Tests		Direct Compression			Overall compression.

* Traverse gauge measurements were made over certain parts of the wing after buckling.

4. *Method of Test.*—4.1. *Loading Rig.*—For purposes of test, the specimen complete with the attachments described in section 2.3 was mounted horizontally in the test frame. The starboard end (Fig. 7) was supported on single pin joints at the fore-and-aft ends of the end bulkhead, the pins being arranged chordwise with coaxial centre-lines. These served the double purpose of supporting the weight of the specimen at this end and anchoring this end of the specimen against the torsion loads, the application of which is described below. The weight of the other end of the specimen was counterbalanced by two dead-weighted shot bag cradles attached to the ends of two cables running from the bulkhead members and over pulleys to the carriers. Fig. 7 is a diagram showing the specimen and loading rig, described below, and Fig. 8 is a photograph of the specimen rigged ready for test.

The internal pressure was applied by a compressed air supply coupled to the wing through a reducer valve comprising a large drum with a controlled leak valve. The resulting internal pressure was measured by means of a mercury U-tube manometer attached to a pressure point on the rear web.

The bending load was applied by means of a mechanical straining gear acting through a ' nutcracker ' arrangement of two levers. The load was measured by a 5-ton spring balance fitted into the open end of the nut-crackers.

The torsion load was applied by the application of up-and-down loads to the fore-and-aft ends of the bulkhead at the port end of the specimen. These loads were applied through two skewed levers pulled together at the ends remote from the specimen by a turnbuckle. The resulting load was measured by a hanging weigher. The weight of this, together with the weight of the overhanging lengths of the beams were counterbalanced by shot bags on the end of a cable attached at its other end to the top beam above the weigher.

In all the tests the appropriate loads were applied in increments up to the value given in the table of section 3.3.

4.2. *Description of Measuring Apparatus.*—A photograph showing the various instruments used for measurements of the initial shape of the specimen and the surface distortions under load is shown in Fig. 9. The profile gauge was made from steel plate to fit the true aerofoil section, the profile edges of the gauge being cut to the dimensions aimed at by the firm in making the specimen. Inspection of the gauge after manufacture indicated that the ordinates were all within the limits 0 to + 0·005 in. of the specified values. The gauge was fitted on the specimen and the gap between the gauge and the wing surface measured by means of wedge or feeler gauges. The curvature gauge comprised a grooved bar, two pedestal blocks and a dial gauge which indicated the amount by which the wing surface was offset from a flat surface between the two pedestal blocks. At the chordwise section concerned readings of this gauge were taken as it was moved along the section an inch at a time, the gauge feet being set at 2-in. centres. The traverse gauge consisted of a dial gauge on a mounting block arranged to slide along a graduated straight edge supported on two feet at one end and a single foot at the other.

The dial board comprised a special board supported in pedestal blocks at the front and rear webs and mounting a number of dial gauges arranged to measure the distortion of the top wing surface normal to itself at the crest and trough of each corrugation. Both Figs. 8 and 9 show this board in position on the wing.

The bow or bending deflection at the front and rear webs and the twist of the specimen was measured by six vertical dial gauges mounted on the floor and connected to the webs at the positions shown in Fig. 6. The measurements of the horizontal closure between the end bulkheads were made using dial gauges at various chordwise locations. The final measurements, on which the remarks of section 5.2 were based, were taken at the cast iron attachment brackets above and below the specimen.

4.3. *Method of Testing Panels.*—The two panels were tested in a vertical compression testing machine using the method described in Ref. 5.

5. *Summary of Results.*—The results of the tests are summarized under the same title headings as are used in the table of section 3.3 and are given below.

5.1. *Initial Shape Measurements.*—Fig. 10 shows in diagrammatic form the results of the measurements made with the profile gauge. The results of the measurements made with the curvature gauge are reproduced for the upper surface in Fig. 11, which shows the readings of the dial gauge plotted against the chordwise position of the gauge. No attempt has been made to correct the results to give a true curvature in terms of a radius, as the latest tendency is to compare wing smoothness on the basis of the curvature gauge readings when the feet are set 2 in apart Spanwise waves between corrugations of the order of 0·003 in on 2 in were measured using the traverse gauge. Along the centre-lines of the screws at the crests of corrugations, waves of the order of 0·010 in on 3 in were measured, the waves bulging inwards between internally driven screws. These measurements also indicated that the majority of the externally driven screws either protruded above the skin or were sunk below the skin by some small amount, the average difference in level between the skin and the screw heads being about ± 0·0015 in. The filling over the internally driven screws protruded above the skin in nearly all cases. The average amount of protrusion being about 0·0025 in. Further measurements indicated that the 'step' at the leading-edge skin joint on the top surface averaged 0·002 in. with peak values of 0·006 in. Examination of the bottom surface joint indicated a much better joint from this point of view.

5.2. *Tests on End Conditions.*—Plots of the compression of the specimen at the neutral plane against chord for load factor 2 with bending load only applied, showed that for all practical purposes the end bulkheads remained plane as far as bending about a vertical axis was concerned. Graphs of the angular movement of the ends of the specimen about a chord line plotted against chord indicated that there was a twist between the ends of the bulkheads about a chord line

which increased as the loading point moved forward. From the two sets of graphs mentioned above the graphs of Figs. 12 and 13 were obtained. These graphs show the angular deflection of the end bulkheads in a horizontal plane and the mean twist of the bulkheads, plotted against the chordwise position of the loading point. It will be appreciated that as these two graphs do not cut the chord axis at the same point it would not have been possible to fulfil the ideal condition that there should be no drag bending, and the vertical bending moment should be distributed so as to result in a uniform angular straining of the specimen at all points along the chord. This latter condition is the more important, as the stresses resulting from the vertical bending are much greater than the stresses from the compression and drag bending. The condition would have been fulfilled if it had been possible to load at position B (Fig. 13) when there would have been no twist of the end bulkheads and hence the bending would have been correctly distributed. However, the rig design was such that this was impracticable. It was therefore decided to use, for the remaining tests, Position 1 at 27·14 in aft of the leading edge, as this was the original position chosen for loading before these tests could be made and was also the most convenient from the rigging aspect.

5.3. *Distortion Measurements up to a Factor $n = 2g$.*—The results of the distortion measurements made with the dial board are given in Figs. 14 to 16 presented in three different ways to facilitate analysis. The change in wave amplitude, determined as the difference between the deflection of the skin at the trough of each corrugation and the deflection at the pairs of adjacent crests, was plotted against load factor. From these curves the maximum value of the wave amplitude for each of the chordwise sections was determined: this, plotted against chord, is shown in Fig. 14. It should be noted here that these results are calculated from the difference of two large quantities and cannot be expected to be accurate to more than $\pm$ 0·001 in. Figs. 15 and 16 show load deflection graphs for Corrugation Crests 6, 12 and 18, and curves of corrugation crest deflections against chord respectively for test IV.100; the deflections being relative to the front and rear webs at the sections concerned. These two are typical of similar graphs which were much the same for all the Series A tests.

5.4. *Proof Tests.*—For the purpose of these tests the wave sizes, given in Ref. 3, of 1 in 1,000 chordwise and 3 in 1,000 spanwise were taken as critical from an aerodynamic point of view. Hence, if after a proof loading there was a permanent set in the wave amplitude between corrugation crests of more than 0·0036 in. the ' proof load ' of the specimen would be considered to have been reached.

During the course of the tests a number of minor failures occurred which were repaired between tests. In Test V.100 at a factor of 3·5 a chordwise ridge formed between externally driven screws forward of the rear web. This was found in Test V.200 to be due to failure of the internally driven skin attachment screws by pulling out of the skin. A spanwise traverse of the buckle at factor 3·5 and zero load indicated a permanent wave of 5 in 1,000 spanwise. In spite of this exceeding the critical value test work was continued in order to obtain as much information as possible. An attempt was therefore made to repair this damage by inserting external screws to replace the failed self-tapping screws. This met with little success and further similar buckles occurred at a factor of 3·5 in Test V.300. Consequently all the internally driven screws in the upper surface of the specimen were reinforced by two No. 6 Parker-Kalon hardened self-tapping screws, type Z6, of length 0·5 in, located to either side of the internal screws and $\frac{3}{4}$ in apart. This reduced the maximum screw pitch spanwise from $1\frac{1}{2}$ in to $1\frac{1}{8}$ in. A further minor failure occurred at factor 4 in Test V.400 due to fracture of the screws attaching the D-nose to the front web. Extra screws were inserted. After none of these tests did the permanent set in the wave amplitude exceed the critical value except in the region of the first chordwise buckle. It was not until after Test V.500, in which the load was taken to factor 5, that the set in wave amplitude exceeded the critical value. After this test the set was 0·0095 in between corrugation crests at one position and 0·0036 in in many other places.

The shapes of the graphs of corrugation crest deflection against chord, at factors greater than about 3, were very irregular, a typical example being reproduced in Fig. 17 for factor 5 in Test V.500.

Graphs of the bend offset and the twist of the specimen over the test length for Tests V.400 and V.500 showed slight signs of yielding of the specimen above factor 3·5 to 4·0.

5.5. *Ultimate Test.*—At a factor of 4 in this test distinct waviness of the surface was apparent, chiefly concentrated round the screwheads. As the load was increased this waving developed until at a factor of 5 there was considerable ' inter-rivet ' buckling between the screws forward of the rear web, and there were indications of screws failing. This buckling increased in severity until finally at a factor of 5·85 the specimen failed by an instability failure of the skin and corrugations at the position where the initial damage had occurred in Test V.100. As the specimen failed to take further load the test was stopped. Fig. 19 shows a view of the failure and Fig. 18 graphs of the bend offset and torsional deflection of the specimen over the test length.

Examination of the failure after test indicated that the ridges of the chordwise skin and corrugation buckles were parallel but offset from one another. This is illustrated by the photograph of Fig. 20 of the small panel cut from the specimen in the region of failure. It was found that the 7 4 B.A. $\frac{1}{4}$-in. long screws inserted during the proof tests had all pulled out of the corrugation crests. None of the Parker-Kalon type Z6 screws, inserted later in the proof tests, had failed.

Control tests on the material of the skin and corrugations were made by the Materials Department, R.A.E., and the results were as follows.

	Material from Corrugation	Material from Skin	Specification Minimum DTD.390
Limit of Proportionality	9·0 t/sq in	9·5 t/sq in	—
0·1 per cent Proof Stress	19·3 ,,	20·4 ,,	15 t/ sq in
Maximum Stress	27·7 ,,	27·0 ,,	25 ,,
Modulus of Elasticity $E \times 10^{-6}$ lb/in^2 ..	9·8	10·2	—
Elongation of 2 in. per cent	23	19	15

5.6 *Results of Panel Tests.*—On the first panel, which was cut from an undamaged part of the top surface, slight buckling of the centre panel became apparent at a mean stress of 3 t/sq in, but this was not permanent until a stress of 11 t/sq in. was reached. Final failure occurred at a stress of 12·2 t/sq in. by severe buckling of the skin followed by local buckling of the corrugations along a line across the panel. The load *vs* deflection graph for this panel was straight up to a stress of 9·5 t/sq in.

The second panel was cut from the bottom surface of the specimen and had only the internal and external screws at 1·5-in pitch attaching the skin to the corrugations. Load was applied until the skin buckled away from one row of internally driven screws. This occurred at a stress of 5·2 t/sq in. The panel was then repaired in the same way as the top surface of the wing had been repaired after initial failure in Test V.100, using one line of short 4 B.A. screws in tapped holes. In this way it was hoped to reproduce the type of failure which had occurred on the wing where these screws had pulled away from the corrugations. However this was not successful, and final failure occurred by a ridging of the skin and corrugation flanges on a line away from these screws, none of which pulled out. The ultimate stress reached was 11·7 t/sq in, whilst the load deflection graphs were straight up to a stress of 9·8 t/sq in.

A discussion of the panel test results and a comparison between the ultimate stresses reached in the wing test and in the panel tests are given in section 9.2.

PART II

Comments on the Aerodynamic Efficiency of the Wing

6. *Aerodynamic Efficiency of the Wing after Manufacture.*—6.1. *Discussion of Wind-tunnel Tests.*—The wind-tunnel tests made on the specimen at the National Physical Laboratory, indicate that at Reynolds numbers up to about $5 \cdot 5 \times 10^6$ extensive laminar boundary layers and low drag coefficients were obtained with this specimen. At higher Reynolds numbers there was an appreciable increase in drag coefficient attributed to the increased effect of the tunnel turbulence. Hence the true behaviour of the aerofoil at higher Reynolds numbers has not been determined by direct aerodynamic measurement. As, however, the Reynolds number of this section at 10,000 ft at its design maximum level speed of 330 m.p.h. E.A.S. is 18×10^6, it is necessary to find some estimate of its efficiency at this number. This can only be done by a consideration of the smoothness of the specimen in the light of the available information on this subject.

6.2. *Comments on the Initial Shape.*—Regarding the general deviation in shape illustrated by the full and broken lines shown on the full-scale section in Fig. 10, this amounts to a very slight change in camber of the aerofoil. Such a change might affect the lift and pitching-moment curves for the wing but these do not concern us here. The effect on the drag coefficient is considered to be negligible.

Turning next to the local buckling or ridging of the specimen, the ideal limits for the amplitude-wave length ratio of spanwise and chordwise ridges are 1 in 1,000 and 3 in 1,000 respectively. Spanwise buckles of wave lengths greater than 6 in can be assessed from the profile gauge measurements with a fair degree of accuracy. It will be seen from Fig. 10 that on the top surface there is an indentation of about 6 in 1,000 with its centre at corrugation trough number 1. An indentation almost as severe occurs on the lower surface in a similar position. Both these are also indicated by the discontinuous change in the curvature gauge readings around this region (Fig. 11) where the width of the band enclosing curvature gauge readings exceeds the ideal limit used so far of 0·005 in (for a 2-in setting of the gauge feet). These and the traverse gauge measure ments indicate that the wing was not quite as smooth as would be liked. The 6 in 1,000 indentation is not so serious as it would appear, as its length chordwise was 9 in and it was well faired in with the rest of the surface.

The ideal to be aimed at with protrusions, like filling over the screws, has not been fixed very definitely as yet, but the maximum height should not exceed 0·0005 in. About 40 per cent of the screws inserted internally had a filling over them which protruded by about 0·002 in. Hence, as a protruding head affects a wedge-shaped area behind it with a 20 deg apex these protrusions would quite possibly disturb the laminar flow at the higher Reynolds numbers. No comments are made on the effect of the externally inserted screws. These were not intended to be 'smooth' as they were inserted after the wind-tunnel tests The step at the leading-edge skin joint also averaged 0·002 in compared with the ideal value of something between 0·0002 and 0·0005 in. Hence the same remarks apply to this as to the screw protrusions.

7. *Ability of Wing to Resist Flight Loads.*—7.1. *Distortion up to* 2*g.*—The remarks to be made in this and the next section will be based on the assumption that the distortion tests were made on a perfectly smooth specimen. In other words any distortions occurring during testing will not be added to those already present initially as would occur in practice. In this way it will be possible to discriminate between the suitability of the type of construction from the viewpoint of ease of manufacture to the required smoothness and its ability to resist distortion under service conditions.

From the wave amplitude summary graph of Fig. 14 it will be seen that only near the rear web and at corrugation trough number 11 in the pressure test did the amplitude exceed the critical value of 0·0036 in (1/1,000 × 3·6, distance between corrugation crests). As transition would occur at the rear spar in any case due to the adverse pressure gradient there, these results are good. The specimen should satisfy the condition that it must remain smooth at its maximum level speed with small manoeuvring and gust accelerations superimposed. Further it is of interest to note from the graphs of Fig. 14 and still further supported by the graphs of Fig. 15, that if the specimen is satisfactory in maximum level flight at $n = 1g$, then provided the speed does not increase the smoothness will remain much the same as the factor increases to $2g$.

7.2. *Proof Loadings.*—With the wing in the condition as received for loading tests the proof load factor would only be 3·5 or 58 per cent. of the design ultimate factor, as the internally inserted screws failed at this load and there was excessive permenent buckling. Upon repairing the wing by decreasing the effective screw pitch from 1·5 in (or 3 in considering the internally inserted screws ineffective) to 1·125 in this factor was increased to 5·2. This is nearly 90 per cent of the design ultimate factor which is the proof load percentage normally used in strength tests.

It will be appreciated that the screws used for the repairs are not satisfactory from the smoothness aspect as they need careful countersinking and filling flush with the skin. These were only used to expedite the repair work. It is understood that for future smooth wing work the firm propose to use countersunk rivets with the heads ground flush with the skin. Provided these are placed at about 1-in pitch they should be satisfactory.

Further comments on the proof factor achieved will be found in Part III under structural efficiency.

PART III

Comments on the Structural Features of the Wing

8. *Skin Distortions under Load.*—8.1. *Local Distortion between Corrugations.*—The local distortion of the skin between corrugations is of primary importance and therefore warrants careful consideration. The graphs of wave amplitude of Fig. 14 show features of particular significance which are summarized below :—

(a) The superposition of the bending and torsion loads, applied separately or together, on the pressure loading has a small effect on the maximum wave amplitude. It will be seen from Fig. 14 that in general the increase is from about 0·0010 in to about 0·0013 in, except in the region of the front and rear webs. A large increase would not be expected, as the compression and shear stresses at $2g$ loading are well below the buckling stresses.

(b) Over the majority of the wing, after the $1g$ loading has been reached the wave amplitude tends to remain constant or if anything to decrease. This can be explained by the remarks made above in (a) combined with the fact that above $1g$ loading the pressure, the primary cause of these deflections, remains constant.

(c) At the corrugation trough adjacent to the rear web the wave amplitude is in all cases negative except for Station B on the rib centre-line. This would suggest that where the web is unsupported by rib or stiffener it transmits a fixing moment to the adjacent portion of the skin through the web flange. This would account for the negative wave-amplitude, corresponding to inward buckling, and also for the fact that in the combined pressure, bending and torsion test, when the web buckling was most severe, the wave amplitude reached its highest negative value at this position. It should be noted that this effect would be unlikely to occur on a complete wing as there would be no normal pressure on the web.

For a comparison of the wave amplitude with theory the skin between corrugations may be considered as having clamped edges, and elementary beam theory may be used. The central deflection of such a beam under a uniformly distributed load may be expressed as :—

$$h = 0{\cdot}0315\frac{pL^4}{Et^3},$$

where p = normal pressure, t = plate thickness.
L = width between supports,

Now, for a pressure of 170 lb/sq ft, the pressure at $n = 1g$, the above formula gives a value for h of 0·0013 in compared with a measured value of 0·001 in at this pressure in Test I.100 (pressure only). In Fig. 14 it will be seen that the wave-amplitude was some 30 per cent. greater in the tests with bending or torsion applied as well as pressure than in the test under pressure only.

Graphs of wave amplitude, not reproduced in this report, show that this varies quite widely between the various corrugations and chordwise between the various sections. It is quite probable that this is due to the effect of the internal stresses induced in the skin when the specimen was made. The bending stress in the skin under a normal pressure of 170 lb/sq ft is only 0·5 t/sq in. This is well within the order of stress which may be present initially.

8.2. *General Distortion of Skin and Corrugations.*—The general distortion of the top skin panel between the front and rear webs is illustrated by the graphs of Fig. 16. It is difficult to explain the curious ' dip ' or minimum in these graphs, especially as it was apparent even in the tests under pressure only.

9. *Comparison of the Failing Load with Theory.*—9.1. *Initial Failure in Proof Tests.*—In Test V.100 the failure was due to inter-rivet buckling on a pitch of 3 in due to the internally inserted screws being virtually ineffective. Based on the section modulus of the wing, considering the skin fully effective, the stress at the factor of 3·5g was 6·64 t/sq in. Stressed-skin data sheet 02.01.10 gives an inter-rivet buckling stress of 7·4 t/sq in. for a rivet pitch of 3 in. The slightly higher value given by the data sheets may be explained by the fact that inter-rivet buckling stress is very sensitive to the distance between the rows of rivets. This is apparently not allowed for in the data sheets. In the wing the rows were very close together, compared with normal practice.

9.2. *Ultimate Failure.*—Practically all the design data available on the strength of corrugated construction is based on empirical rules deduced from panel tests. The ultimate strength of the wing, will therefore be compared with the results of the tests on the panels cut from the wing itself.

Using simple bending theory and assuming the top skin of the wing as being fully effective, the stresses in the top surface of the wing at failure were:—

Compression stress = 11·1 t/sq in
Torsion stress = 2·43 t/sq in

The mean failing stress of the panels, 12·0 t/sq in, was corrected to allow for the presence of shear stress by using a similar expression to that deduced in R. & M. 1965[4] for initial buckling under combined shear and compression. Instead of using the buckling stresses in the formula

$$\frac{\sigma}{\sigma cr} + \left(\frac{\tau}{\tau cr}\right)^2 = 1, \quad \ldots \quad \ldots \quad \ldots \quad \ldots \quad \ldots \quad \ldots \quad (4)$$

the ultimate stresses were used giving

$$\frac{\sigma}{\sigma_{ult}} + \left(\frac{\tau}{\tau_{ult}}\right)^2 = 1 , \qquad (5)$$

where τ = the shear stress in panel,

τ_{ult} = ultimate shear stress for panel when the compressive stress is zero (taken as 10 t/sq in, the initial buckling load for simply supported edge condition),

σ = the ultimate compressive stress for the panel when the shear stress is τ,

σ_{ult} = the ultimate compressive stress when the shear stress is zero (taken as 12·0 t/sq in).

This gave a corrected compression failing stress for the panels of 11·3 t/sq in. which compares very well with the compression stress in the wing at failure of 11·1 t/sq in.

It is of interest to compare the stress at which inter-rivet buckling occurred in the ultimate test with the value given by the stressed-skin data sheets. On the wing the inter-rivet buckling was not definite in form until a factor of 5 was reached, when the compressive stress was 9·5 t/sq in. based on the full area modulus. The stressed skin data sheets give for a rivet pitch of 1·125 in an inter-rivet buckling stress of 12·2 t/sq in.

9.3. *Reduction of Ultimate Load for Material Properties.*—From the results of the control tests given in Section 5.5 it will be seen that the 0·1 per cent proof stresses of the skin and corrugation material were 29 to 36 per cent above specification. Conventionally speaking, therefore, the ultimate factor of the wing should be divided by 1·3 to give the ultimate factor of a wing with material on the minimum specification limits.

10. *Conclusions.*—The chief difficulty in the production of a smooth wing having thick skin reinforced with corrugations would, from the work reported here, appear to be that of making the wing sufficiently smooth in the first instance, Provided this difficulty can be overcome the wing should remain smooth under the loading imposed in service.

From the design aspect the waving between corrugations can be calculated with sufficient accuracy from the formula

$$h = 0{\cdot}0315 \frac{pL^4}{Et^3} ,$$

and considering only the pressure loading, the increase due to bending and torsion not being appreciable. The strength can be estimated by comparison with panel tests. The panel test results should be compared with the compression stress obtained from simple bending theory, assuming the top skin fully effective. Should the shear stress in the skin be large the panel stress result should be further corrected by a formula of the type

$$\frac{\sigma}{\sigma_{ult}} + \left(\frac{\tau}{\tau_{ult}}\right)^2 = 1 .$$

REFERENCES

No.	*Author*	*Title, etc.*
1	E. J. Richards, W. S. Walker and J. R. Greening.	Drag Tests on Samples of Laminar-flow Wing Construction (1) Armstrong-Whitworth. A.R.C. 6436. January, 1943.
2	—	Design Requirements for Aeroplanes. A.P. 970, Chap. 203.
3	D. M. A. Leggett	Data for the Design of Smooth Wing Surfaces. R. & M. 2193. January, 1944.
4	H. G. Hopkins and B. V. S. C. Rao ..	The Initial Buckling of Flat Rectangular Panels under Combined Shear and Compression. R. & M. 1965. March, 1943.
5	E. A. Brock	The Behaviour in Compression of Aluminium Alloy Panels having a Flat Skin with Corrugated Reinforcements. A.R.C. 9013. July, 1945. (To be published.)

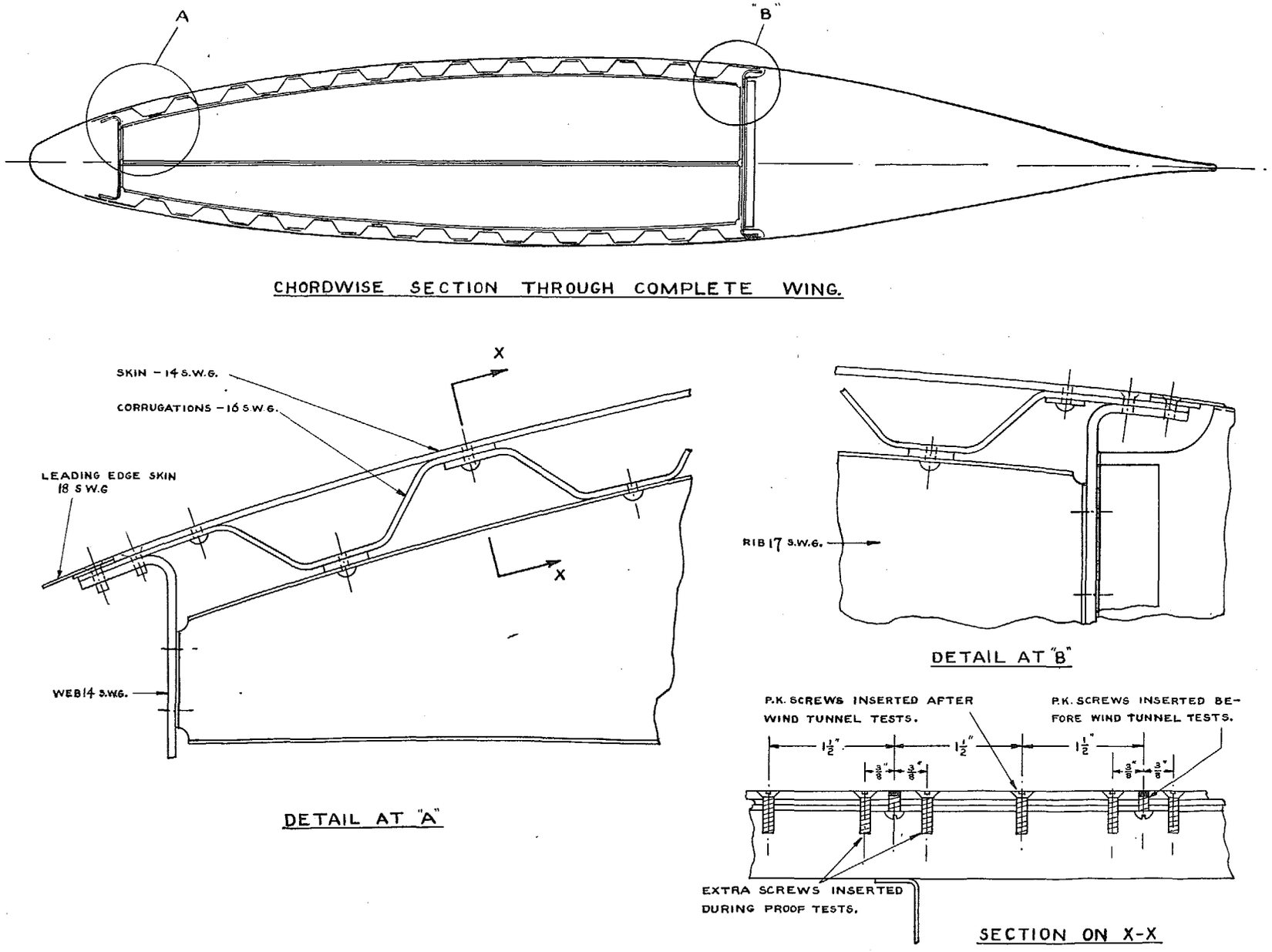

FIG. 1. Sectional Views of Armstrong-Whitworth 6 ft. Chord Smooth Wing Specimen.

a) PRELIMINARY BENDING OF SHEET.

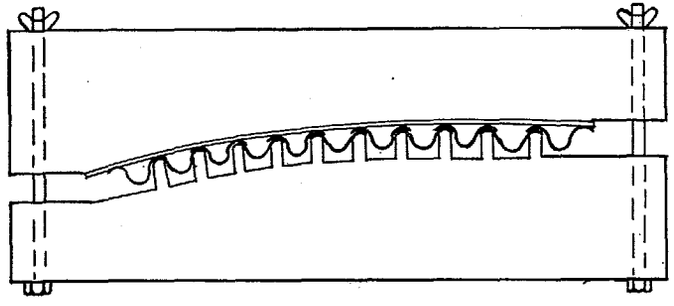

b.) ASSEMBLY OF SHEET AND CORRUGATIONS IN JIG.

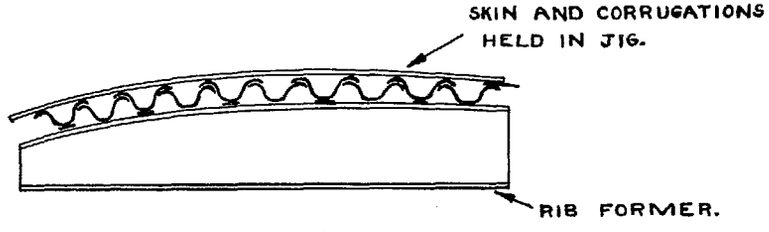

c.) ASSEMBLY OF RIB FORMERS.

FIG. 2. Method of Manufacture.

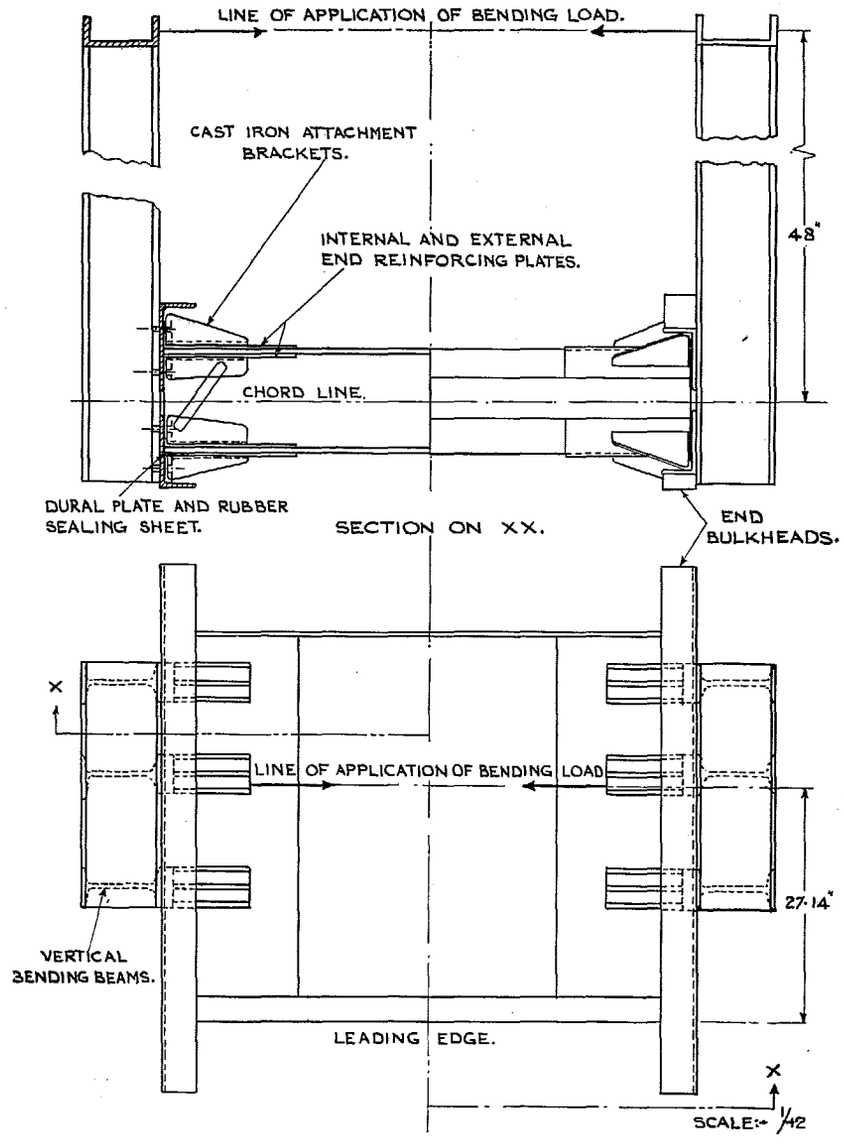

FIG. 3. Loading Attachments on Specimen.

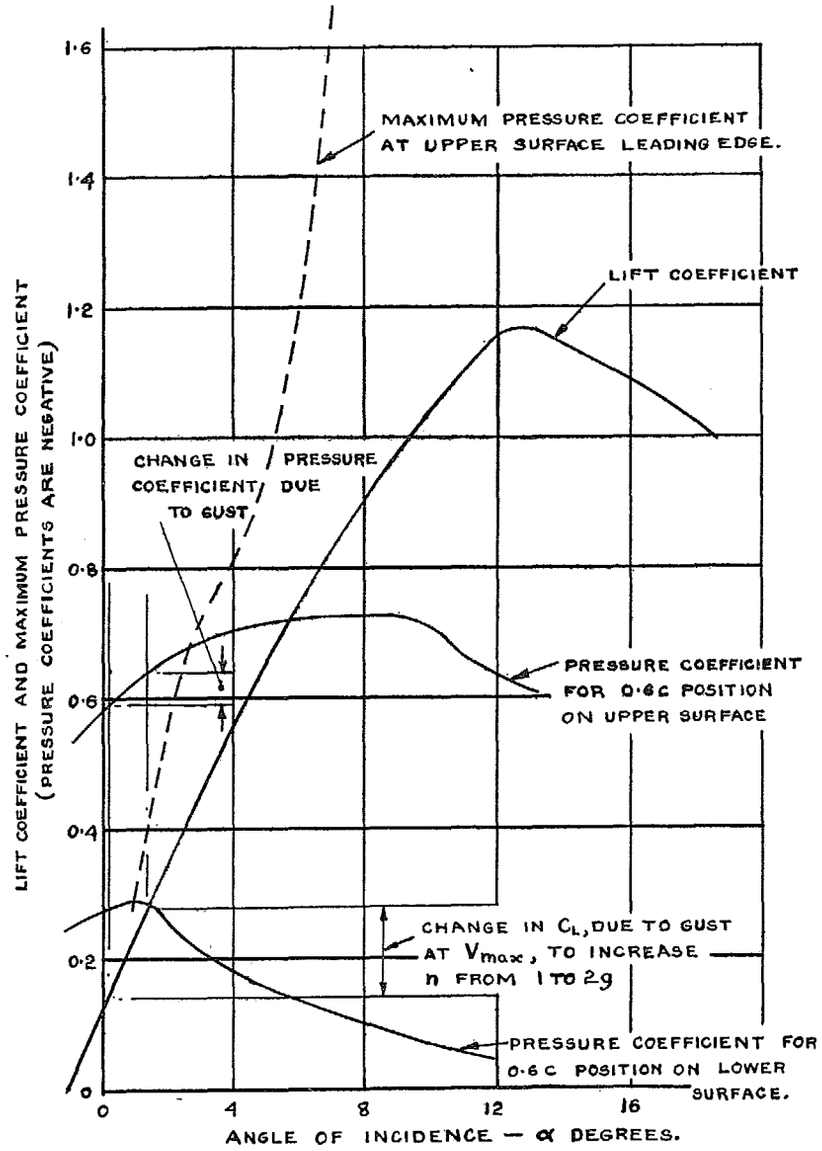

FIG. 4. Lift and Pressure Coefficient Curves for NACA 66–2–216 Section.

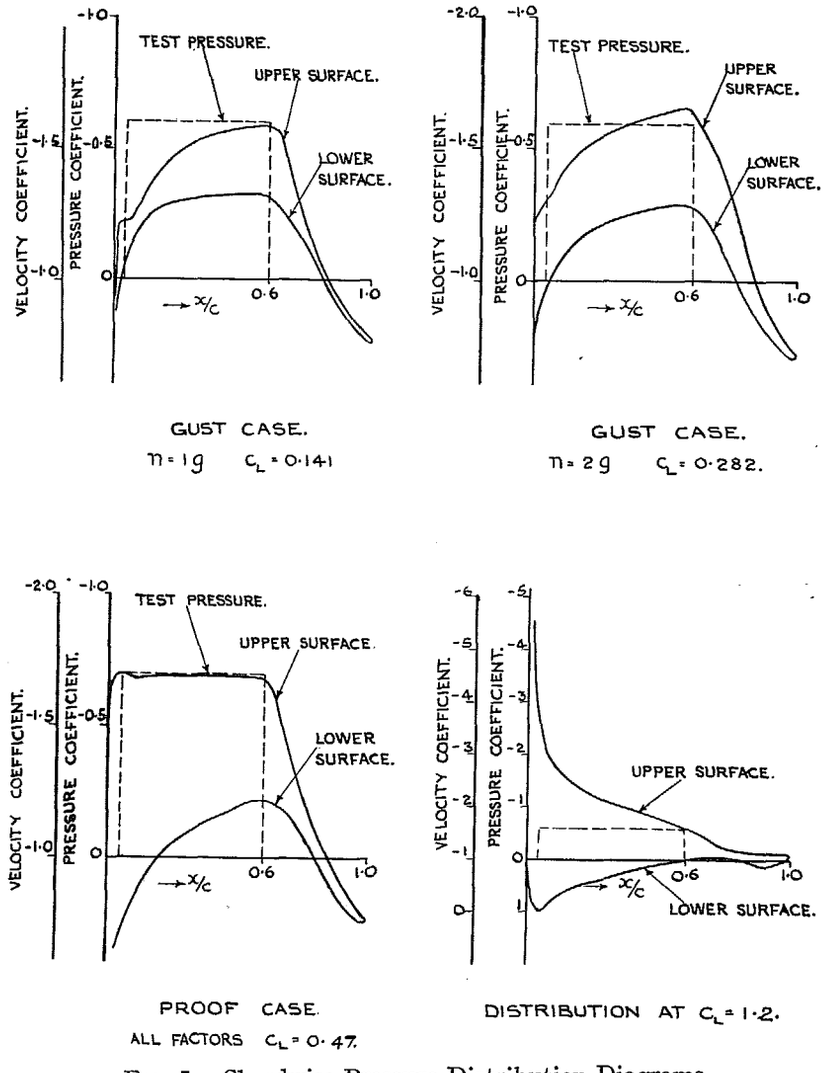

FIG. 5. Chordwise Pressure Distribution Diagrams.

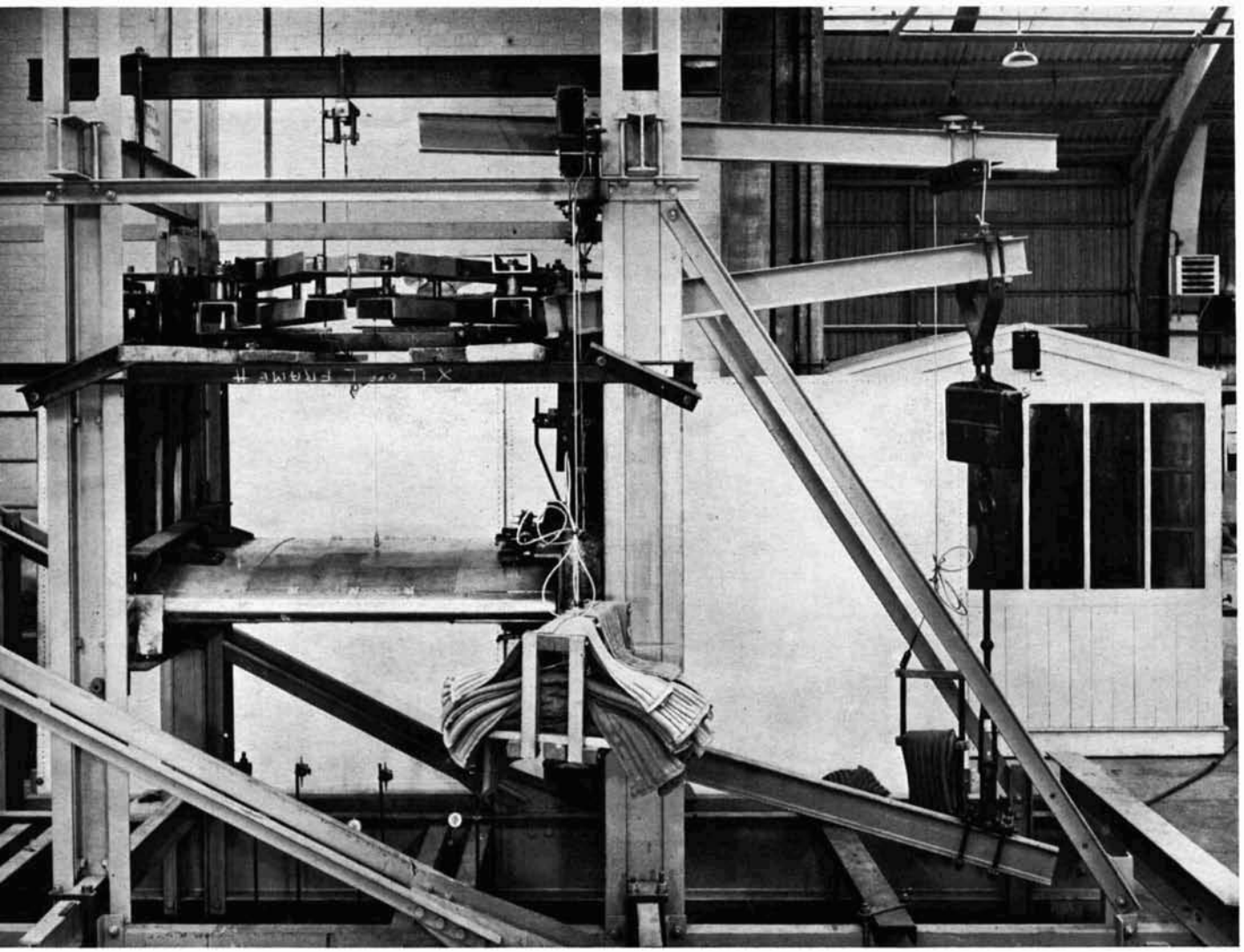

FIG. 8. Front View of Specimen in Test Frame.

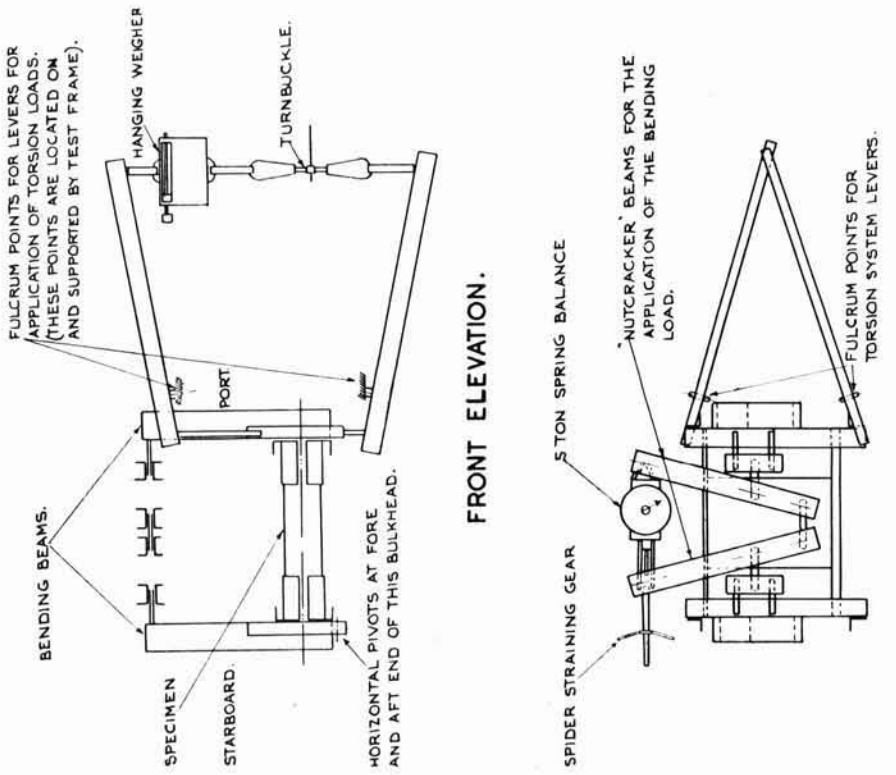

FIG. 7. Diagram showing Loading Rig for Test.

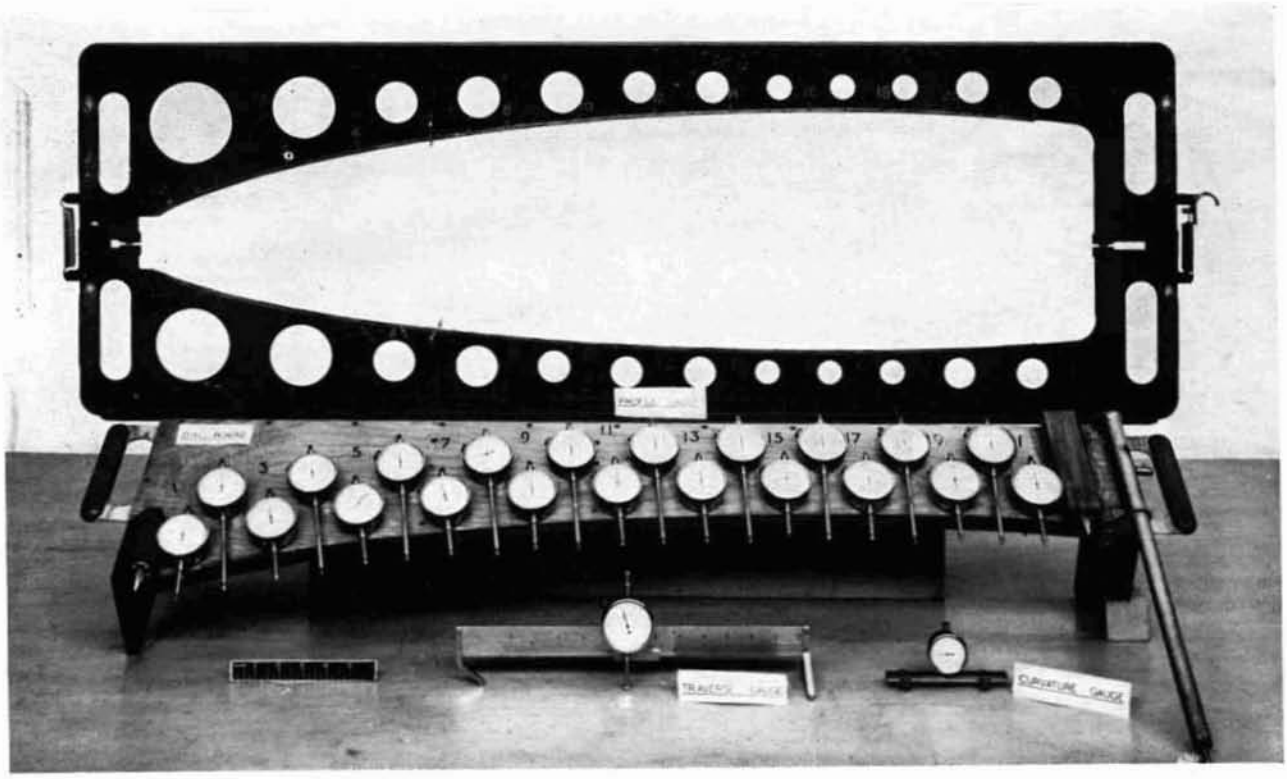

FIG. 9. Smooth Wing Measuring Instruments.

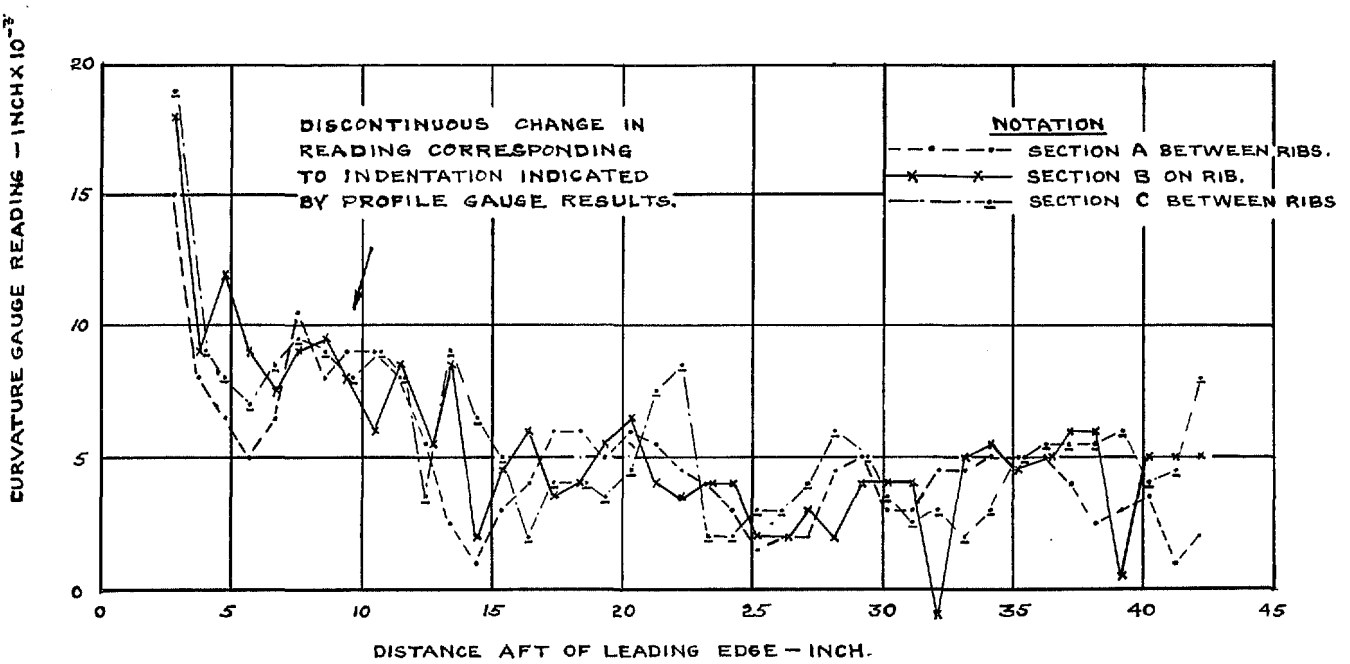

FIG. 11. Graphs of Curvature Gauge Readings against Chord for Sections A, B and C, Upper Surface, before Loading Tests.

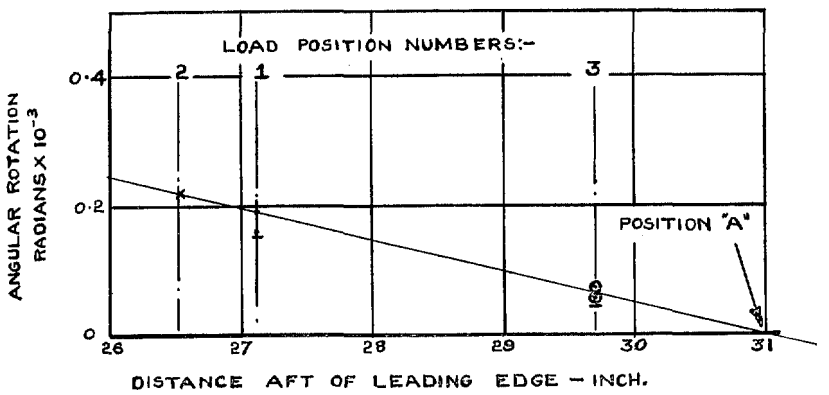

FIG. 12. Graph of Angular Rotation between Ends of Specimen—about Vertical Axis against Chordwise Position of Loading Point.

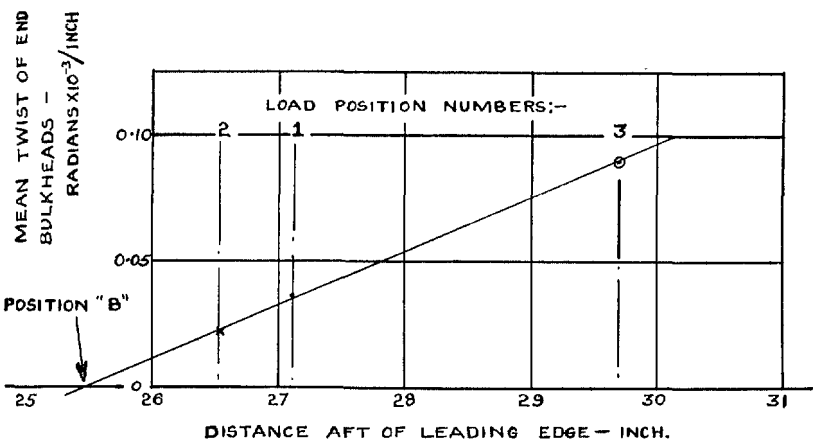

FIG. 13. Graph of Twist of End Bulkheads against Chordwise Position of Loading Point.

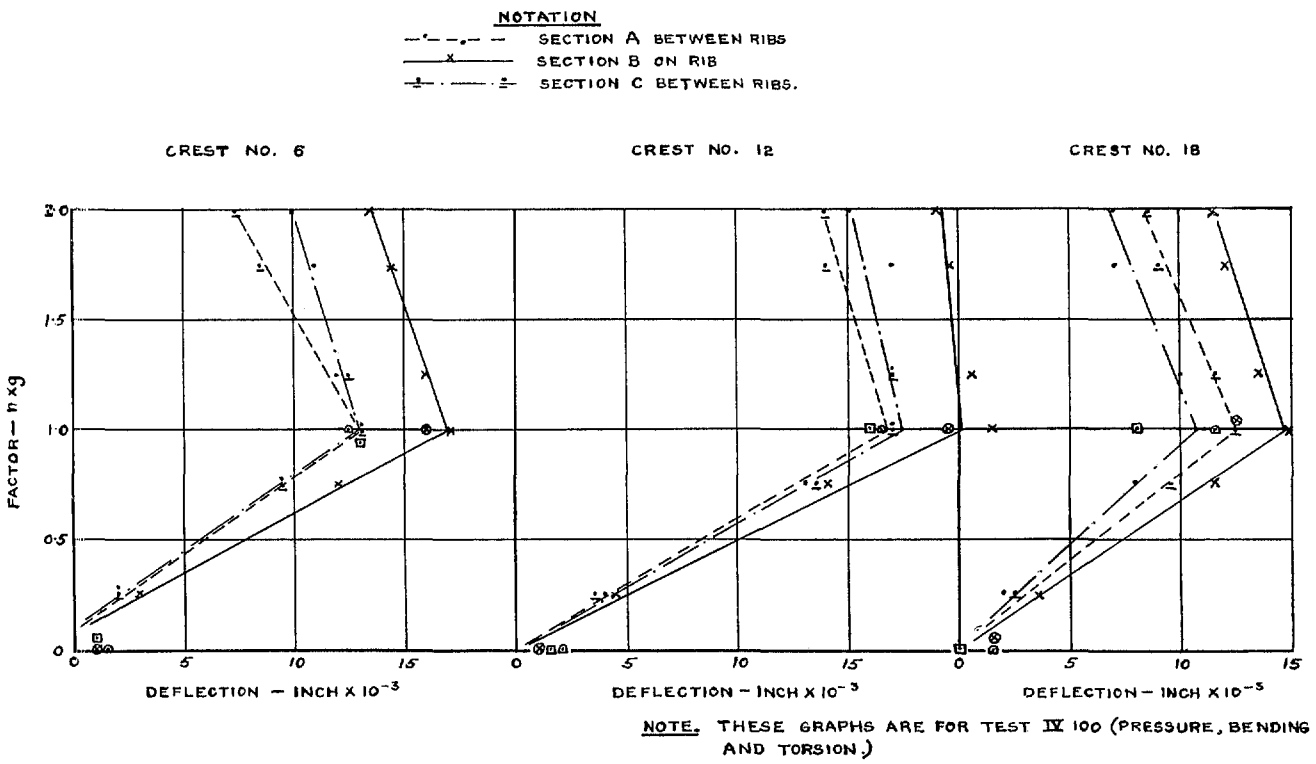

FIG. 15. Load Factor—Deflection Graphs for Corrugation Crests Nos. 6, 12 and 18.

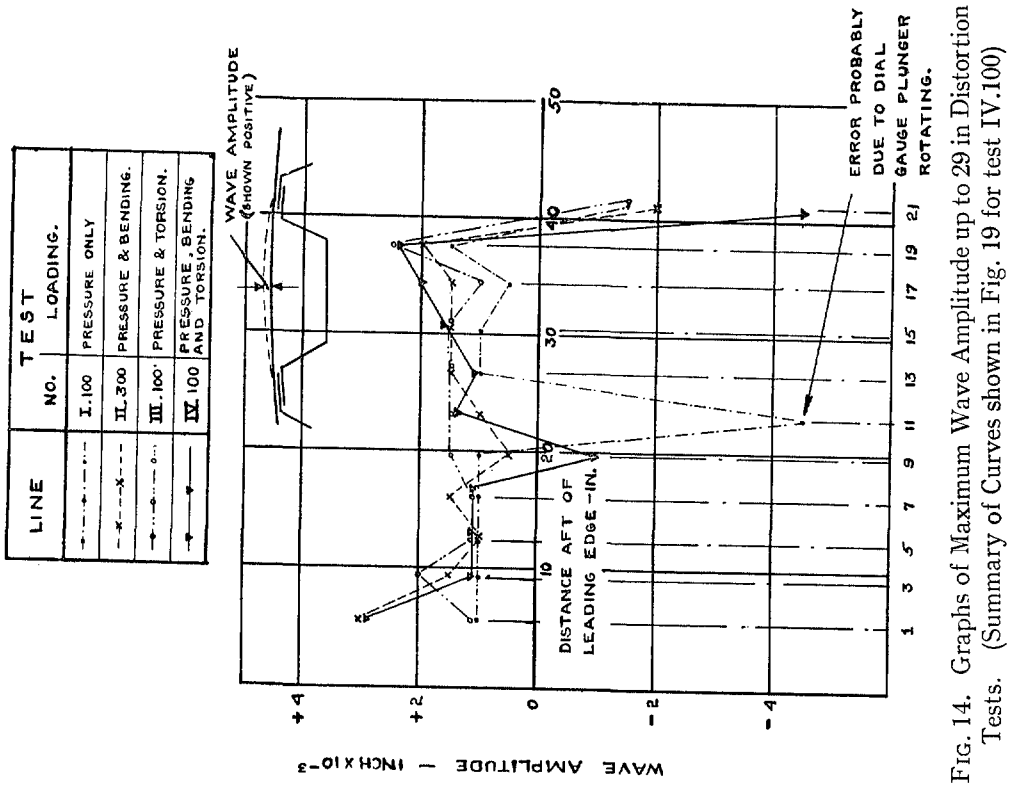

FIG. 14. Graphs of Maximum Wave Amplitude up to 29 in Distortion Tests. (Summary of Curves shown in Fig. 19 for test IV.100)

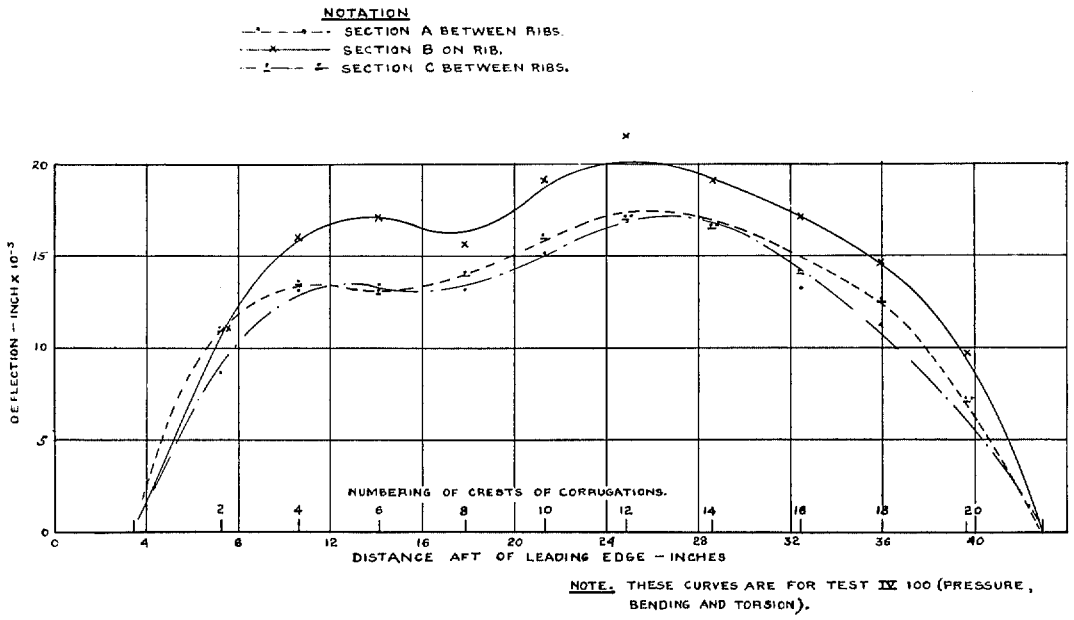

FIG. 16. Deflections Plotted Chordwise for Sections A, B and C at Factor $n = 1g$.

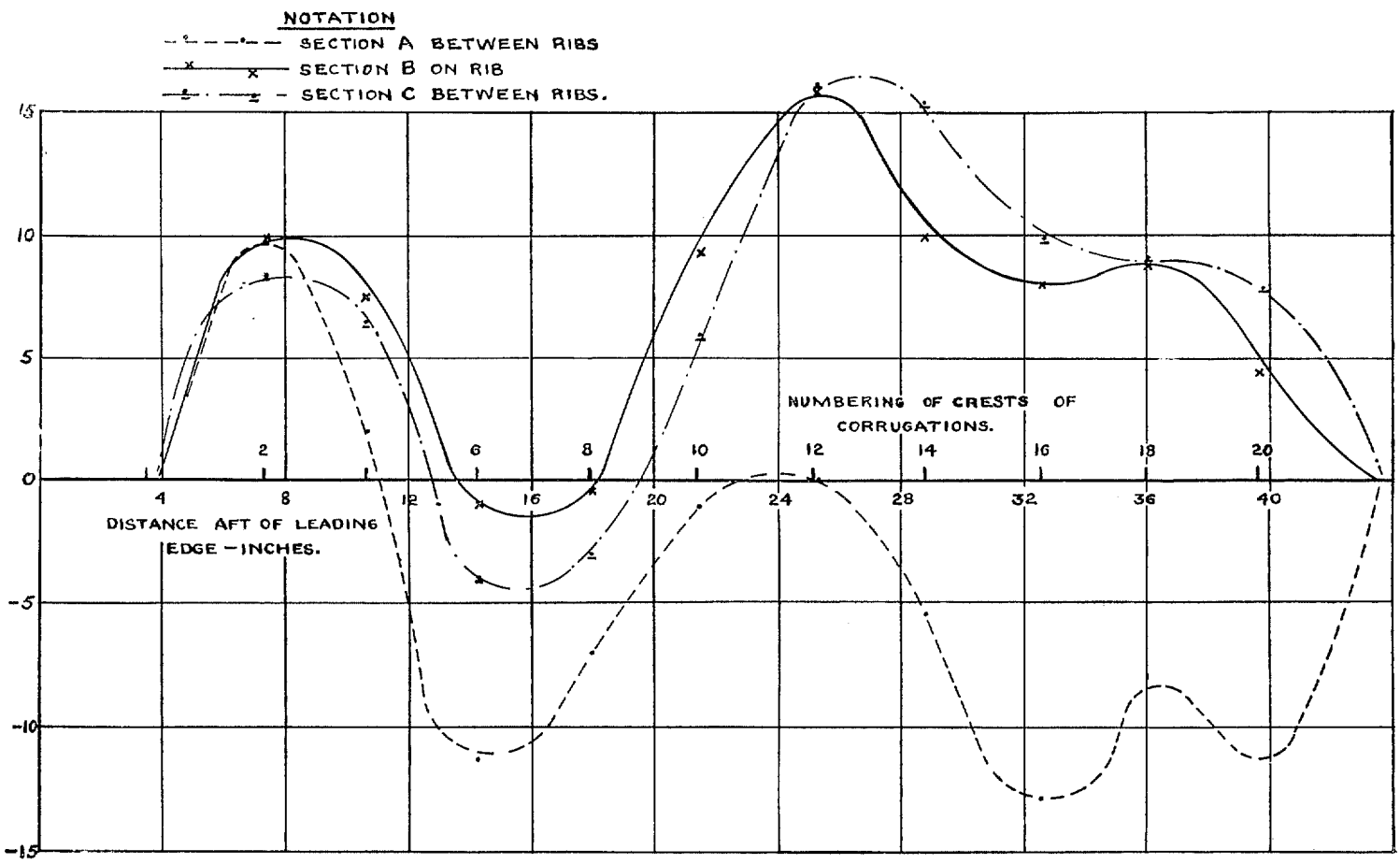

FIG. 17. Deflections Plotted Chordwise for Sections A, B and C and Proof Test V.500 at $n = 5g$.

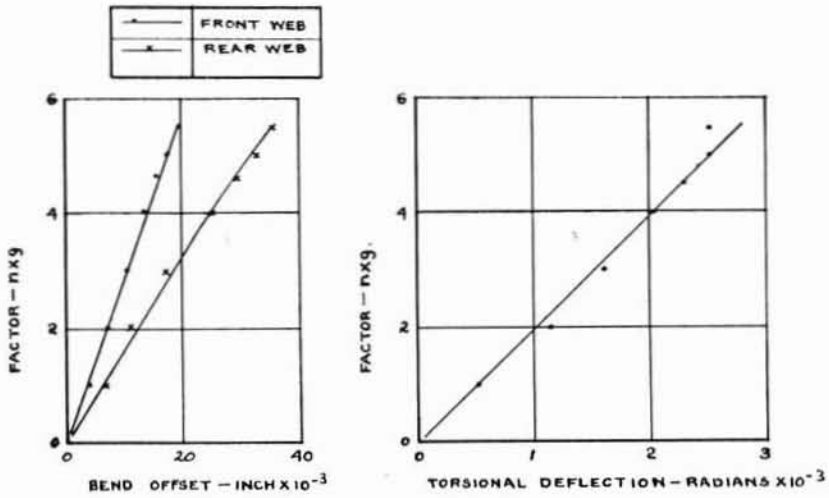

FIG. 18. Specimen Deflections in Ultimate Test VI.100

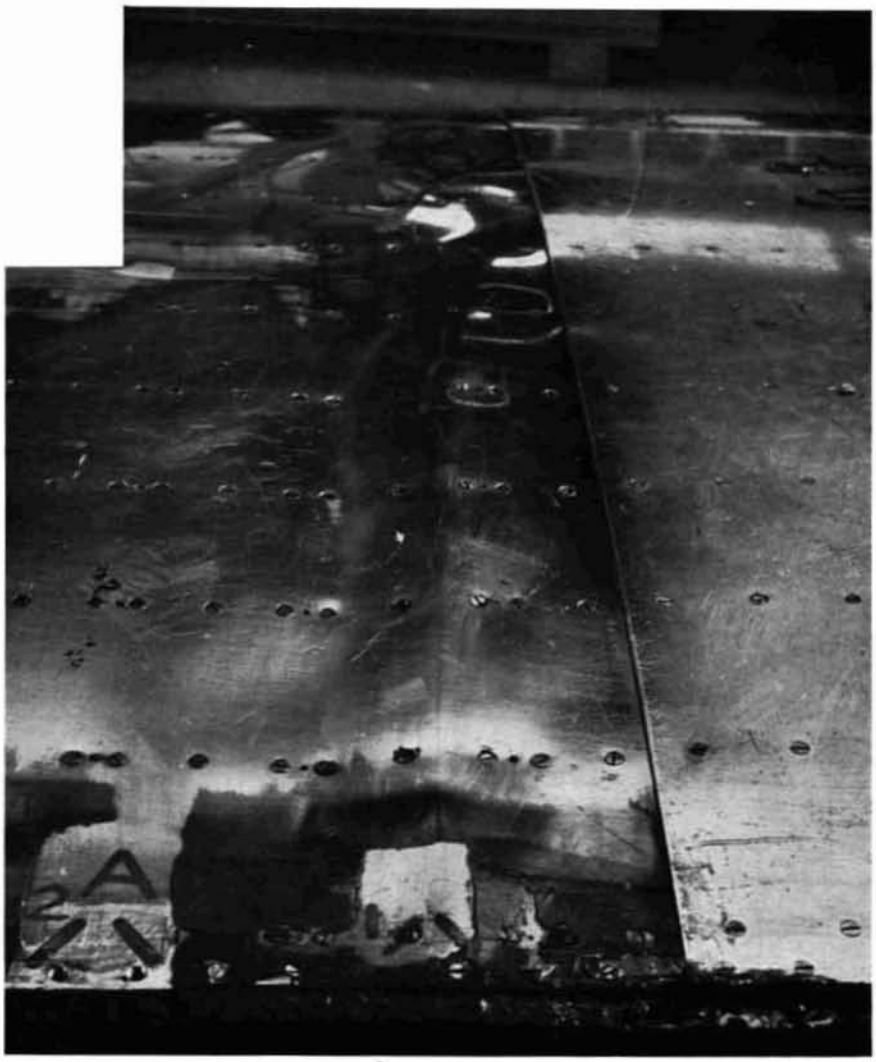

FIG. 19. View of Chordwise Skin Buckle at Position 1 (after test).

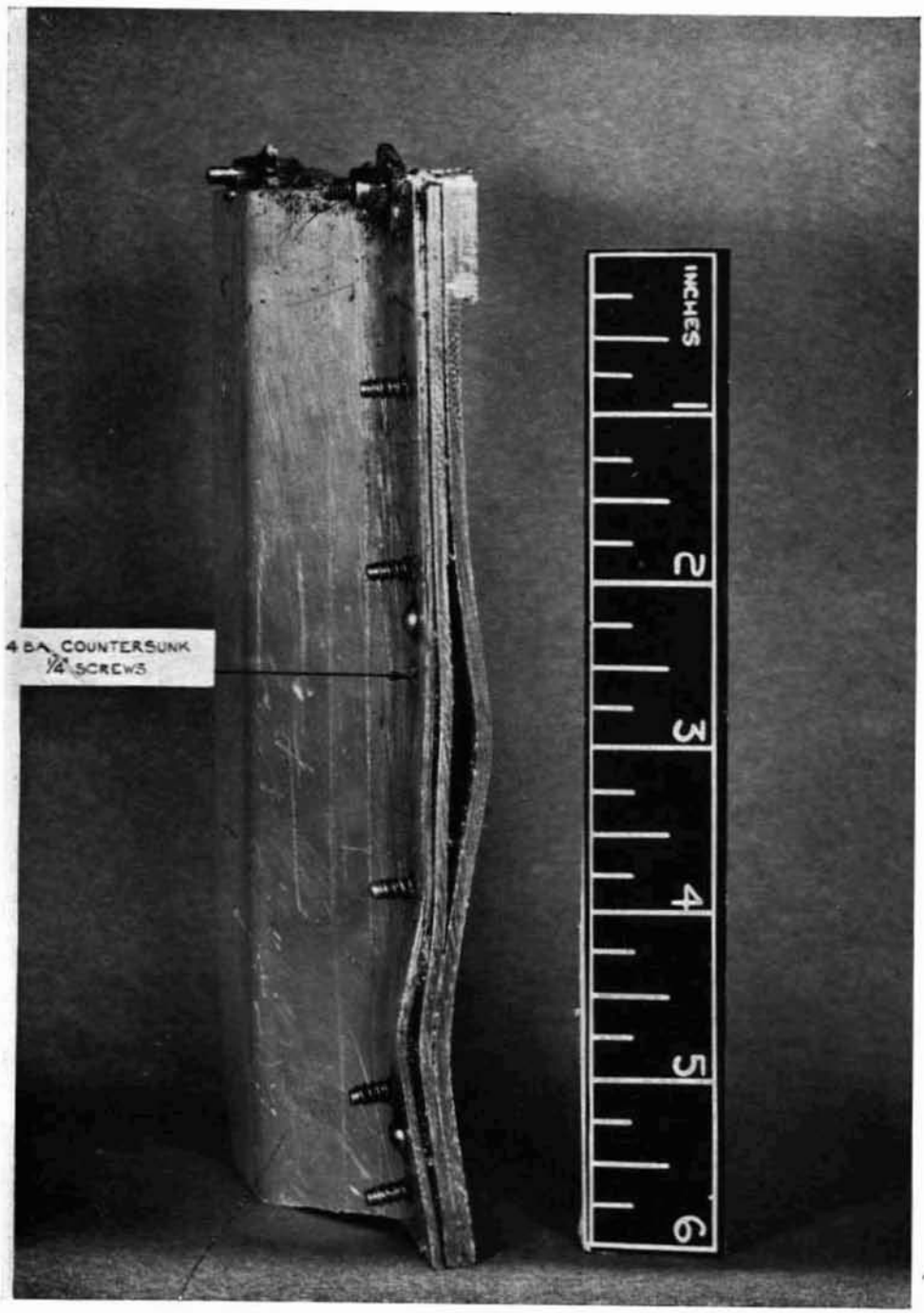

FIG. 20. End View of Panel Cut from Top Surface of Specimen.

(93258) Wt. 13/806 K.5 6/51 Hw.

PRINTED IN GREAT BRITAIN

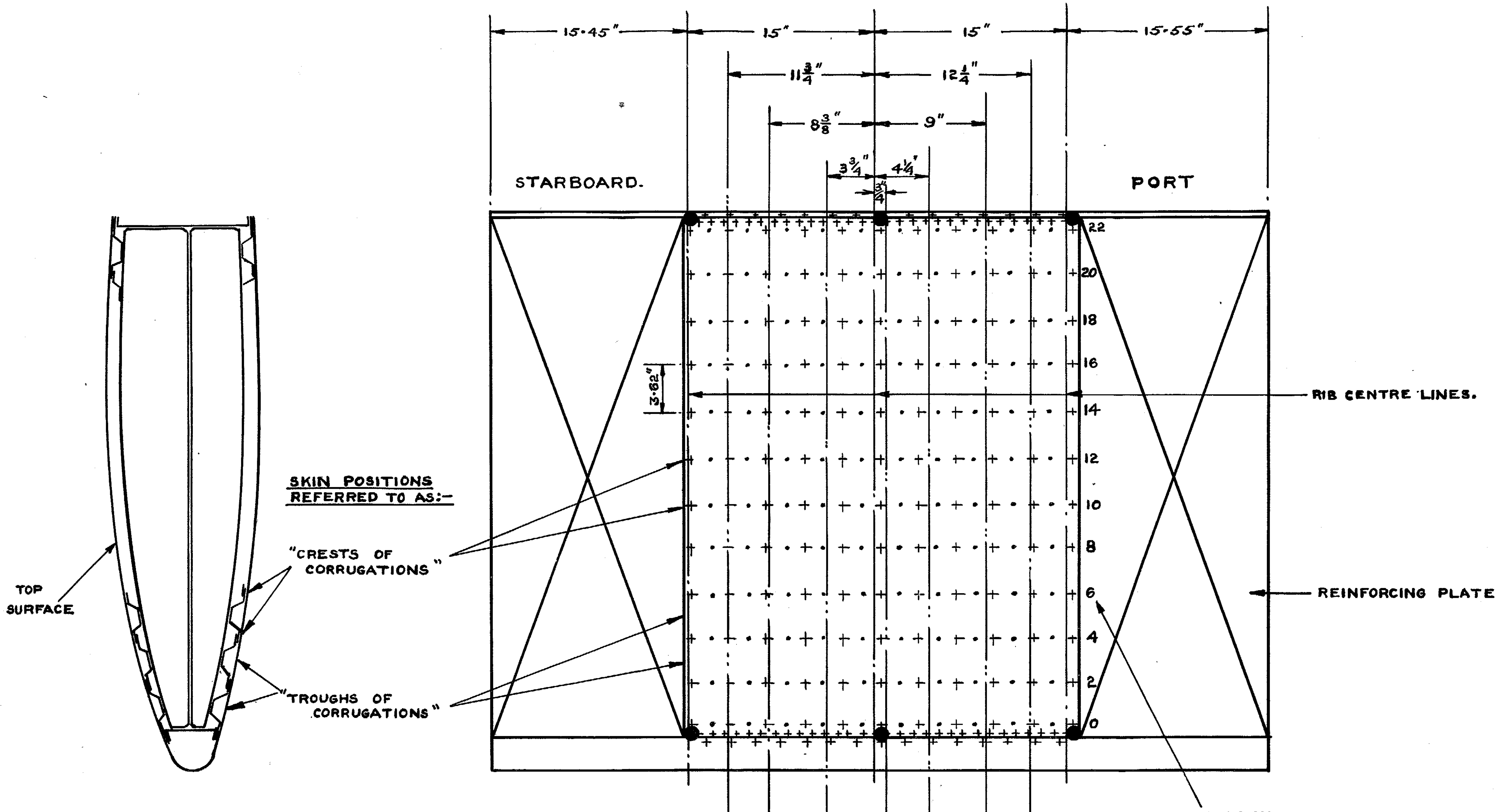

NOTES:- 1) • INDICATES SCREWS INSERTED INTERNALLY DURING CONSTRUCTION
+ INDICATES SCREWS INSERTED EXTERNALLY. THOSE ON THE CRESTS OF THE CORRUGATIONS WERE INSERTED AFTER THE WIND TUNNEL TESTS.
2) DETAILS OF THE SCREW POSITIONS ON THE REINFORCED PART OF THE SPECIMEN ARE NOT GIVEN.
3) ● - INDICATE POSITION OF VERTICAL DIAL GAUGES.

SUBSIDIARY CHORDWISE MEASURING SECTIONS.		1	2	3	4	5	6	7
PRINCIPAL CHORDWISE MEASURING SECTIONS.			A		B		C	
NOTATION USED ON ALL GRAPHS FOR SECTIONS A, B AND C.	LOADING							
	UNLOADING							

FIG:- 6

KEY DIAGRAM SHOWING LOCATION OF MEASURING SECTIONS AND NOTATION USED ON GRAPHS.

A6825 Wt.13 625 3/50 Gp.959 Fosh & Cross Ltd., London

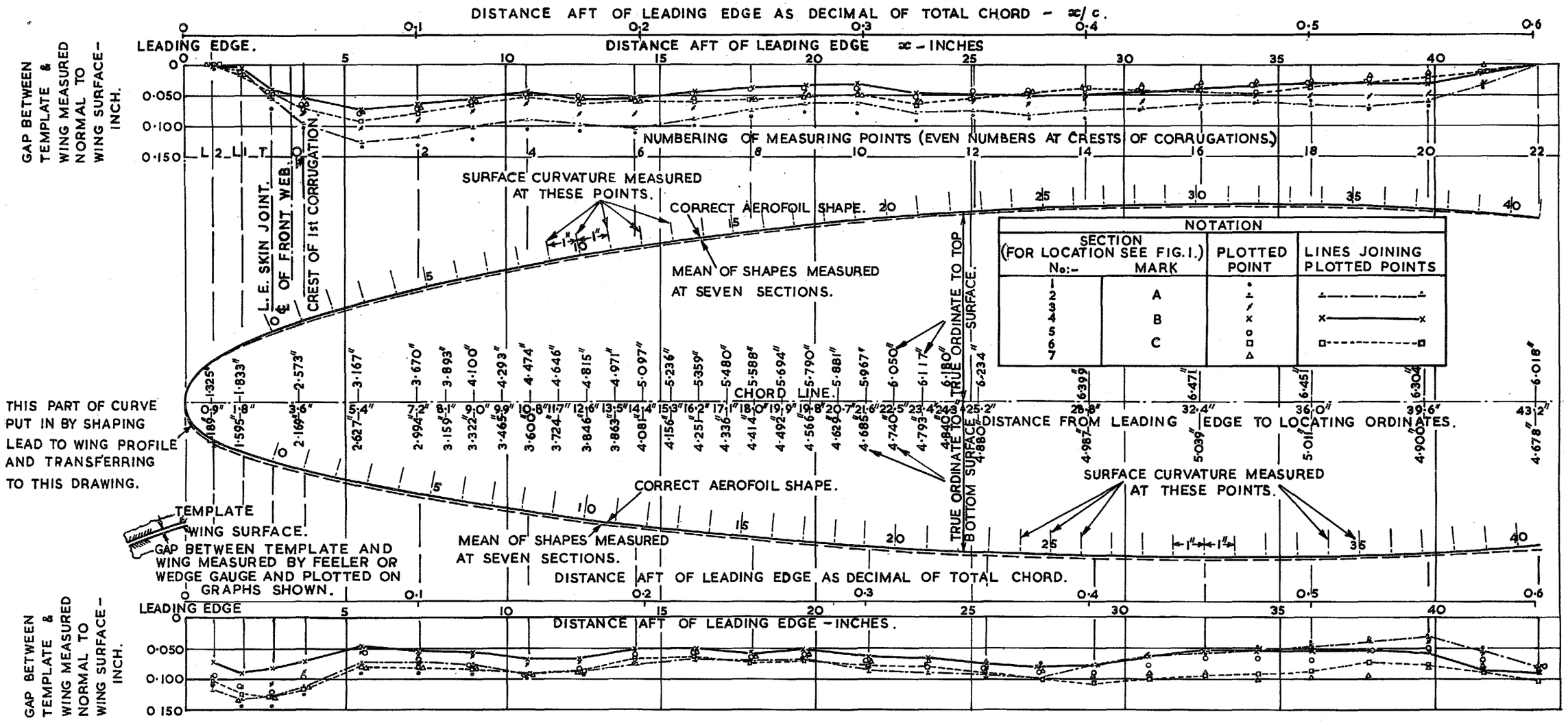

Fig. 10. Full-scale Wing Section and Measurements of Gap between Wing and Template.

A6825 Wt.13 625 3/50 Gp.959 Fosh & Cross Ltd., London

Publications of the Aeronautical Research Council

ANNUAL TECHNICAL REPORTS OF THE AERONAUTICAL RESEARCH COUNCIL (BOUND VOLUMES)—

1934–35 Vol. I. Aerodynamics. *Out of print.*
Vol. II. Seaplanes, Structures, Engines, Materials, etc. 40*s.* (40*s.* 8*d.*)

1935–36 Vol. I. Aerodynamics. 30*s.* (30*s.* 7*d.*)
Vol. II. Structures, Flutter, Engines, Seaplanes, etc. 30*s.* (30*s.* 7*d.*)

1936 Vol. I. Aerodynamics General, Performance, Airscrews, Flutter and Spinning 40*s.* (40*s.* 9*d.*)
Vol. II. Stability and Control, Structures, Seaplanes, Engines, etc. 50*s* (50*s.* 10*d.*)

1937 Vol. I. Aerodynamics General, Performance, Airscrews, Flutter and Spinning. 40*s.* (40*s.* 10*d.*)
Vol. II. Stability and Control, Structures, Seaplanes, Engines, etc. 60*s* (61*s.*)

1938 Vol. I. Aerodynamics General, Performance, Airscrews 50*s.* (51*s.*)
Vol. II. Stability and Control, Flutter, Structures, Seaplanes, Wind Tunnels, Materials. 30*s.* (30*s.* 9*d.*)

1939 Vol. I. Aerodynamics General, Performance, Airscrews, Engines. 50*s.* (50*s.* 11*d.*)
Vol. II. Stability and Control, Flutter and Vibration, Instruments, Structures, Seaplanes, etc. 63*s.* (64*s.* 2*d.*)

1940 Aero and Hydrodynamics, Aerofoils, Airscrews, Engines, Flutter, Icing, Stability and Control, Structures, and a miscellaneous section. 50*s.* (51*s.*)

Certain other reports proper to the 1940 *volume will subsequently be included in a separate volume.*

ANNUAL REPORTS OF THE AERONAUTICAL RESEARCH COUNCIL—

1933–34	1*s.* 6*d.* (1*s.* 8*d.*)
1934–35	1*s.* 6*d.* (1*s.* 8*d.*)
April 1, 1935 to December 31, 1936.	4*s.* (4*s.* 4*d.*)
1937	2*s.* (2*s.* 2*d.*)
1938	1*s.* 6*d.* (1*s.* 8*d.*)
1939–48	3*s.* (3*s.* 2*d.*)

INDEX TO ALL REPORTS AND MEMORANDA PUBLISHED IN THE ANNUAL TECHNICAL REPORTS, AND SEPARATELY—

April, 1950	R. & M. No 2600.	2*s.* 6*d.* (2*s.* 7½*d.*)

INDEXES TO THE TECHNICAL REPORTS OF THE AERONAUTICAL RESEARCH COUNCIL—

December 1, 1936 — June 30, 1939	R. & M. No. 1850.	1*s.* 3*d* (1*s* 4½*d*)
July 1, 1939 — June 30, 1945.	R. & M. No. 1950.	1*s.* (1*s.* 1½*d.*)
July 1, 1945 — June 30, 1946.	R. & M. No. 2050.	1*s.* (1*s* 1½*d*)
July 1, 1946 — December 31, 1946.	R. & M. No. 2150.	1*s.* 3*d* (1*s* 4½*d.*)
January 1, 1947 — June 30, 1947.	R. & M. No. 2250.	1*s.* 3*d* (1*s* 4½*d.*)

Prices in brackets include postage.

Obtainable from

HIS MAJESTY'S STATIONERY OFFICE

York House, Kingsway, LONDON, W.C.2 429 Oxford Street, LONDON, W.1
P.O. Box 569, LONDON, S.E.1
13a Castle Street, EDINBURGH, 2 1 St. Andrew's Crescent, CARDIFF
39 King Street, MANCHESTER, 2 Tower Lane, BRISTOL, 1
2 Edmund Street, BIRMINGHAM, 3 80 Chichester Street, BELFAST

or through any bookseller.